CHARACTERIZATION OF GAMMA-GLYCINE CRYSTALS GROWN IN AQUEOUS SOLUTION OF CEROUS CHLORIDE

M. Josephine Gladiya[1*], G. V. Anuradha[2], V. Sivashankar[3], B. Helina[4]

Article History: Received: 21.05.2023 **Revised:** 30.06.2023 **Accepted:** 26.07.2023

Abstract

The gamma-glycine crystals are the efficient tools for today's optoelectronic and photonic device fabrication as well as for NLO applications. A novel gamma-glycine (GG) crystal was grown by adapting conventional slow evaporation method at room temperature by using aqueous solution of cerous chloride. XRD studies were performed for grown crystal to identify the crystal structure. Functional groups are confirmed by the FTIR analysis and the optical parameters for the grown gamma-glycine crystal are found by recording UV- Vis spectrum. Hardness parameters were found out by Vickers microhardness testing. The elemental analysis for the GG crystal is confirmed by EDAX spectrum. The TG/DTA analysis was carried out for the sample to check the thermal stability. The nonlinear optical activity is confirmed by Second Harmonic Generation (SHG) analysis. The antibacterial activity analysis, cyclic voltammetric and impedance studies of the sample were also carried out and the results are discussed.

Keywords: Gamma-glycine, FTIR, XRD, PL, NLO, TGA, EDAX, impedance, antibacterial activity.

[*]Research scholar, Reg No: 20211282132008
[1,3,4]Department of Physics, St. Xavier's College (Autonomous), Affiliated to Manonmaniam Sundaranar University, Tirunelveli - 627 002, Tamilnadu, India.
[2]Department of Physics, Sri Parasakthi College for Women (Autonomous), Affiliated to Manonmaniam Sundaranar University, Courtrallam, Tenkasi – 627 802, Tamilnadu, India.

Email: [1]josephinegladiya21@gmail.com

DOI: 10.31838/ecb/2023.12.6.243

1. Introduction

Admirably, the amino acids possess astonishing NLO properties[1]. The nonlinear optical materials are the fascinating materials as they plays a prominent role in various fields such as optoelectronic, photonic, fibre optic computing and many other fields[2]. Glycine is the Researcher's delight as it is an stable organic amino acid with single hydrogen atom as its side chain lacking the probability of owing side chain carbon atoms unlike other amino acids, also it is an polar molecule[3,4]. Glycine is uncomplex of all amino acids, with its possibility of existing as trilogy of polymorphic forms ie., (α, β, and γ)[5]. It is pretty apparent that the α and β glycine crystallizes in centrosymmetric space group whereas γ - glycine alone crystallizes in a non centrosymmetric space group, as non centrosymmetric space group solely contributes for NLO property. It is reported that the glycine enhances the property of NLO[6,7].

Pure organic crystals has poor mechanical and thermal properties, while pure inorganic crystals possess low optical non linearity as a result of the lack of π – electron delocalization[8,9]. Semiorganic materials possess greater advantage of having substantial mechanical strength, good chemical solidity, wide transparency in comparision with organic and inorganic crystals because, the organic ligand is ionically bonded with inorganic in the case of semi organic crystals[10]. Past decades crystal growers and Researchers have extensively reported γ - glycine crystals with various combinations such as Sodium acetate, Lithium nitrate, Ammonium sulphate, Potassium nitrate, ammonium oxalate, maleic acid, cadmium chloride etc.,[11-18] and their astonishing properties have been studied by deeper characterization studies.

Main goal of this work is to scrutinize and elucidate the novel γ-glycine single crystal, which has been grown by conventional slow evaporation growth method using the aqueous solution of cerous chloride for the very first time. Herein we report, various parameters such as optical, structural, functional, thermal, mechanical, elemental and electrochemical properties of the grown crystal were interpreted by suitable characterization techniques to exploit and accomplish the liability of the title compound for optoelectronic and photonic applications.

Experimental

A novel γ-glycine single crystals are grown by dissolving high purity glycine and high purity cerous chloride or cerium tri chloride (Cerium III chloride) in a 100 ml of deionised water and stirred in a magnetic stirrer for about 5 hours at a constant temperature of about 50 degrees. The saturated solution is prepared and the solution is then filtered by Whatman filter paper and the perforated vessel is then covered by aluminium foil and left for slow evaporation at room temperature. A good quality single crystal of γ-glycine is grown with the period of 35 days. The grown γ-glycine crystal is shown in fig. 1.

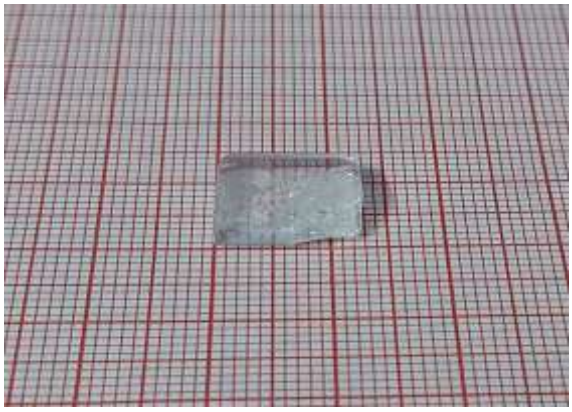

Fig.1: A harvested of single crystal gamma-glycine

2. Results and Discussion

XRD studies

(i) Single crystal XRD study

In order to ascertain the crystal structure and lattice constants, the generated γ-glycine (GG) crystal was subjected to single crystal XRD experiment by utilising a BRUKER D8 QUEST diffractometer with MoK□ radiation (λ=0.71073 Å). According to the findings, the grown crystal's crystal structure is hexagonal, and the information is presented in table 1. Hence, it is found that gamma-glycine is crystallized when alpha-glycine is grown in aqueous solution of cerous chloride.

Table 1: Unit cell parameters of GG crystal

Crystal code	γ-glycine
Crystal System	Hexagonal
□	90˚
□	90˚
□	120˚
a (Å)	7.031(2) Å
b (Å)	7.031(2) Å
c (Å)	5.472(1) Å
V (Å^3)	234.22(2) Å

(ii) Powder XRD study

By using powder XRD method, phase identification, quantitative analysis, and the discovery of structural blemishes have all consistently been accomplished. The powder-XRD technique is widely used in the pharmaceutical industry to identify pharmacological molecules and their polymorphs, and in this study, the polymorph of glycine has been identified[19,20]. The crystallographic characteristics, such as 2θ, d-spacing, relative intensity, and the hkl values, were used to determine the crystalline phase structure of the sample[21]. The d-spacings, analogous to different peak positions were proclaimed by accustomed calculation using $2d \sin\theta = n\lambda$ where θ is the Bragg angle, d is the inter planar spacing, λ is the wavelength of X-rays and n is the order of diffraction. Using a powder X-ray diffractometer (PANalytical XPERT - PRO MPD) with a target of copper, the powder XRD pattern of the gamma-glycine crystal was recorded and it is depicted in figure 2. The three integers h, k, and l (Miller indices) are assigned to each reflection in order to index a powder pattern. For each reflection, the values for h, k, and l are presented in brackets. Making use of the TREOR and INDEXING software tools, the powder XRD pattern's reflections were indexed. It can be shown from the indexing values that the gamma-glycine crystal is a member of the hexagonal crystal system.

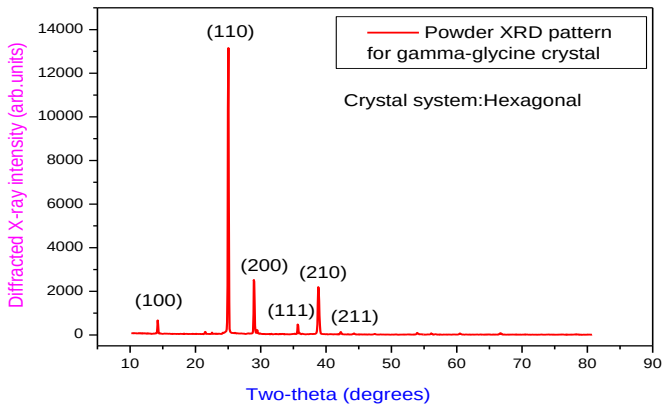

Fig.2: Powder XRD pattern of gamma-glycine crystal

FTIR spectroscopy

The fourier transform infrared spectroscopy is recorded to discover the functional groups present in the grown gamma-glycine crystal. The FTIR spectrum was recorded between 4000 cm^{-1} – 400cm^{-1} using the Perkin Elmer FTIR spectrometer and the recorded spectrum is indicated by Fig:3 . The peak at 3125.71 cm^{-1} corresponds to N-H stretching vibration. Peaks at 2924.09 cm^{-1} and 2172 cm^{-1} corresponds to CH stretching vibration and NH_3^+ assymmetric stretching[22]. Peaks at 1594.63 cm^{-1} corresponds to NH bending and the peak at 1499 cm^{-1} corresponds to weak asymmetric CO_2 stretching[23]. The peak at 1399 cm^{-1} corresponds to COO^- symmetric stretching and the peak at 1334.78 cm^{-1} corresponds to CH_2 wagging. The peaks at 1153.94 cm^{-1} and 1127 cm^{-1} corresponds to NH_3 rocking vibration and NH_3^+ rocking[24]. The peak at 1042.81 cm^{-1} corresponds to CCN asymmetric stretching and 890.33 cm^{-1} corresponds to CCN symmetric stretching. The peak at 929.58 cm^{-1} corresponds to CH_2 rock. The peaks at 607.17 cm^{-1} corresponds to COO^- wagging and 685.86 cm^{-1} corresponds to COO^- bending[25]. Thus,
gamma-glycine crystal was confirmed.

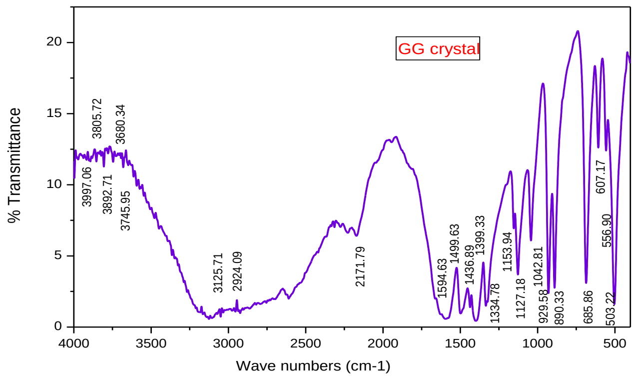

Fig 3: FTIR spectrum of the grown GG crystal

UV-visible spectral characterization

A potent analytical technique for determining the absorption, transmission, and reflectance of a variety of solid and liquid samples in the UV, visible, and near infrared (NIR) wavelength ranges is UV-visible spectroscopy[26]. The type of electrons used in this process is often a valence or bonding electron, which is actuated by the absorption of ultraviolet, visible, or near-infrared light, with the proportion of absorption varies with respect to the wavelength of the radiation and the structure of the molecule[27]. This information is crucial for any NLO material for the reason that it can only be used if it has a wide transparency range, which is inevitable to ascertain its pertinentness for optical applications[28]. These spectra demonstrate how much of the incident light traverse through the sample. Using a Perkin Elmer Lambda 35 spectrophotometer, the UV-visible absorption spectrum of the generated gamma glycine crystal is measured between 200 and 900 nm. The figures 4 and 5 depict the gamma-glycine crystal's absorbance and transmittance spectra. These figures show that the lower cut-off wavelength is 325 nm and that the visible region has low absorbance and high transmittance. The transition and electron delocalization, which are in charge of the nonlinear optical response and UV absorption, are what give rise to the crystal's high UV absorbance. The sample's linear absorption coefficient (□) can be calculated using the transmittance values using the following expression.

$$= [2.303 \log_{10} (1/T)]/ d$$

where T is the transmittance and d is the crystal's thickness. Figure 6 displays the sample's absorption coefficient vs wavelength and illustrates how, in the visible area, the absorption coefficient rises as the wavelength decreases.

The Tauc's plot (Fig. 7), which is created using the Tauc's expression as
□□□□□□□□□□□□□□□□□□□□□□□□□
□□□□□□□□□□□□□□□□□□□□□□□□□
□□□□□□□□□□□□

$$(\alpha h\nu)^2 = A(h\nu - E_g)$$

where E_g is the optical band gap, □ is absorption coefficient, □ is frequency, h is the Planck's constant, and A is a constant, can be used to ascertain the optical band gap value of the sample. The optical band gap of the prepared gamma-glycine crystal is 3.82 eV, as seen in the figure. The extinction coefficient of the grown crystal of gamma-glycine was determined by using following relation

K = □□/4□

Where □□is the wavelength of the light. Figure 8 illustrates the relationship between extinction coefficient and wavelength for the sample. It is obvious that the extinction coefficient value is low at the cut-off wavelength (325 nm) and rises as the wavelength decreases.

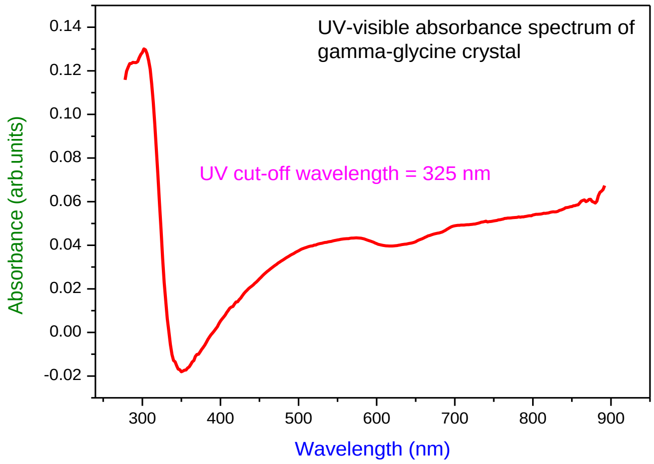

Fig. 4: Absorbance spectrum of gamma-glycine crystal

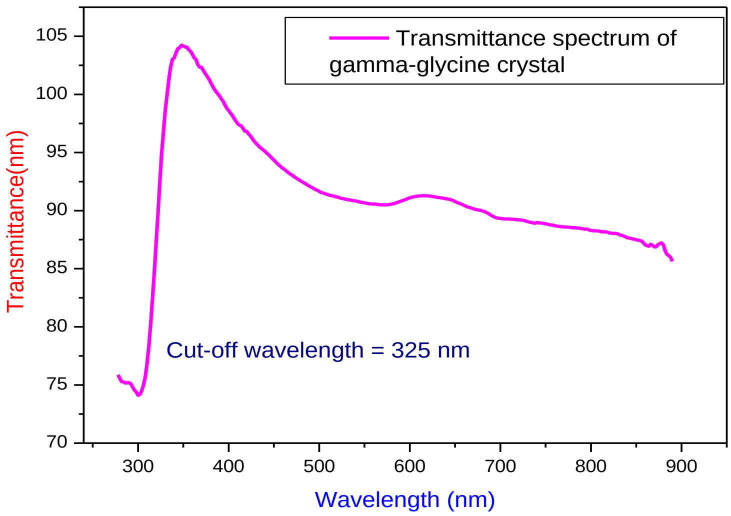

Fig. 5: Transmittance spectrum of gamma-glycine crystal

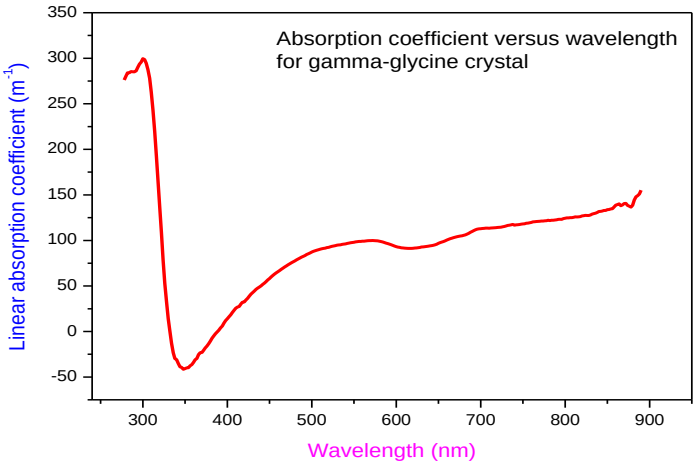

Fig. 6: Plot of linear absorption coefficient versus wavelength for gamma-glycine crystal

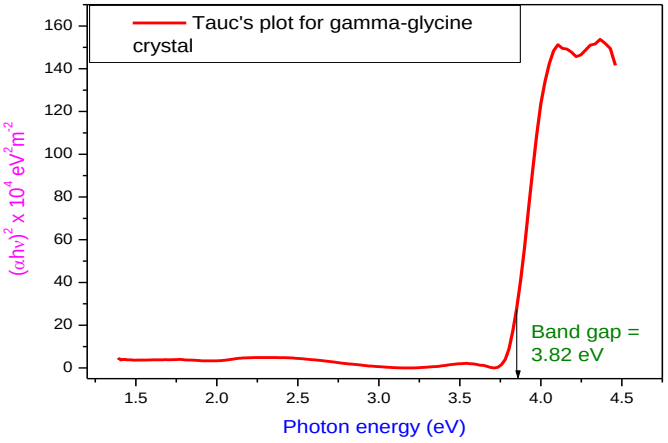

Fig. 7: Tauc's plot for gamma-glycine crystal

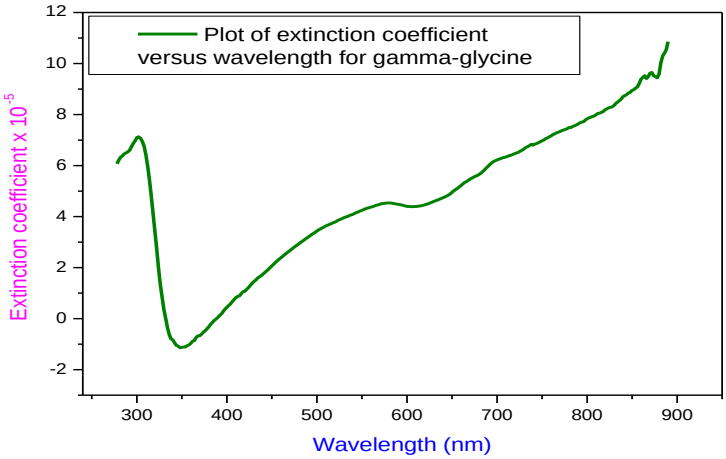

Fig. 8: Plot of extinction coefficient versus wavelength for gamma-glycine crystal Photoluminescence analysis

The photoluminescence analysis is accustomed to study the optical and electronic characteristics of the grown gamma glycine crystal. The spectrum was recorded by making use of a Photoluminescence spectrometer, Flurolog HORIBA. Desirably, UV light activates the sample, that produce the optical radiation in UV, Visible and IR region[29]. The PL emission spectrum of the grown crystal is recorded by exciting a UV light of about 250 nm and the recorded PL spectrum was indicated by the fig: 9. From the spectrum, the emission peaks at 412 nm, 471 nm, 540 nm are in the visible region and 750 nm and 825 nm in the spectrum is due to the emission of IR radiation.

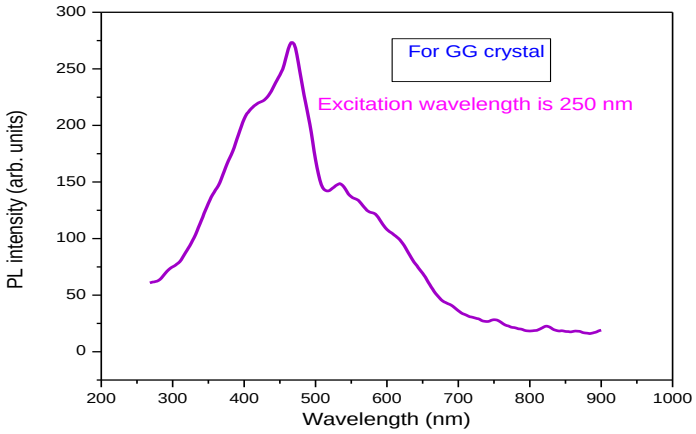

Fig 9: PL spectrum for the gamma-glycine crystal

EDAX spectrum

The stochiometry of the grown crystal was confirmed by the help of Energy Dispersive X ray (EDAX). For the EDAX studies of the grown gamma glycine single crystal, Thermo scientific Apero S, a Hi- Resolution Scanning Electron Microscope (HRSEM) is used. The recorded EDAX spectrum for the grown gamma-glycine crystal is indicated by the figure 10. Initially, the specimen was mounted on a special specimen holder, crystal was examined for EDAX in microscope at various areas to obtain detailed information about the chemical composition[30]. In the spectrum, the C, N and O peaks are approximately at 0.2, 0.3 and 0.4 keV respectively. For a grown single crystal of GG, the atomic distribution of Ce, Cl, C, N and O atoms are 0.24%, 0.98%, 29.22%, 16.39%, 51.62% respectively. Since the title crystal was grown in the aqueous solution of cerous chloride, very small amount of cerium and chlorine are also identified in the crystal.

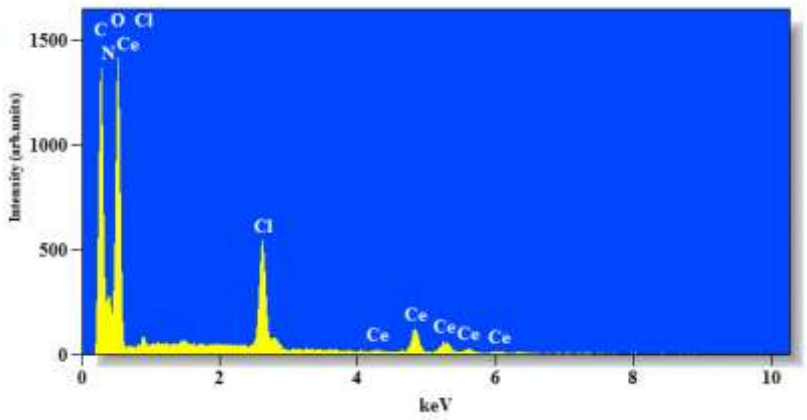

Fig 10: The EDAX spectrum for the grown gamma-glycine crystal

NLO studies

By employing Kurtz and Perry powder technique, NLO efficiency of the sample can be found out. A Q-Switched Nd:YAG Laser (QUANTA RAY MODEL) of 1064 nm was used. Pulse energy of 6 ns and repetition rate of 10 Hz was used. A KDP crystal was used as a reference sample and the output intensity was observed. The input energy of 0.7 J was used and output energy vlaues of green radiation from KDP and gamma-glycine crystal were discovered to be 7.5 mJ and 10.1 mJ. Wavelength of light emitted from the sample was 532 nm. From the result, the NLO efficiency of the gamma-glycine crystal was found to be 1.35 times that of standard KDP sample.

Table 2: Comparision table of SHG efficiency for GG crystal

Sl. No.	Sample Code / Name of the Sample	Output Energy (milli joule)	Input Energy (joule)
1	KDP (Reference)	7.5	0.70
2	Gamma-glycine	10.1	0.70

Microhardness studies

It is well known that the indentation size effect causes hardness in a real crystal to depend on the applied load[31]. Indentation size effects come in two varieties: 1) regular indentation size effect, and (ii) reverse indentation size effect. Reverse indentation size effect (RISE) causes a crystal's hardness to increase as applied load increases, and normal indentation size effect causes a crystal's hardness to decrease as applied load increases[32,33]. The hardness of a perfect crystal will be unaffected by the applied load. Additionally, it is stated that certain NLO crystals exhibit both indentation size effects and that this varies depending on the crystal structure and bonding configurations[34]. For microhardness experiments, the developed crystal of gamma-glycine with flat faces, microscopically free of any evidence of damage, and having approximately dimensions of 3 mm was chosen. A Shimadzu Vickers microhardness tester was used to carry out the experiment. After unloading, the micrometre attached to the microscope eye piece measured the two diagonal lengths of the indentation for each applied load. The variation average diagonal indentation length with applied load for gamma-glycine sample is depicted in the figure 11. The Vickers microhardness number (H_v), which was calculated using the values of d, was then calculated using the formula $H_v = 1.8544\ P/d^2$, where P represents the applied stress and d represents the average diagonal length of the indentation. Figure 12 shows the average diagonal indentation for gamma-glycine crystals as a function of load. The findings reveal that the average diagonal indentation (d) value rises with increasing applied load and exhibits the RISE phenomenon. There is a crack (damage) on the crystal's surface if the applied load is more than 100 g. The crack length is measured from the contact point, and the results obtained are as follows: 32.69 □m and 49.67 □m from the mid-contact point in the left to right direction and 29.97 mm and 45.37 □m from up to down direction from the contact point.

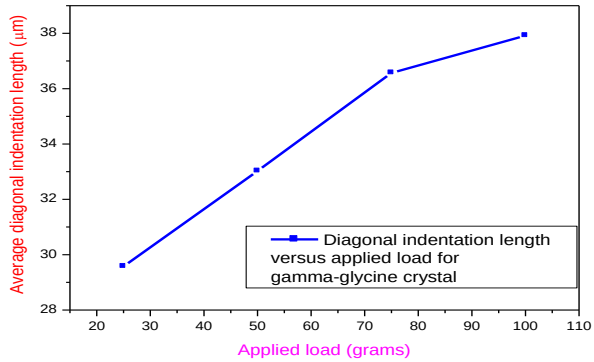

Fig.11: Plot of average diagonal indentation length with applied load for gamma-glycine crystal

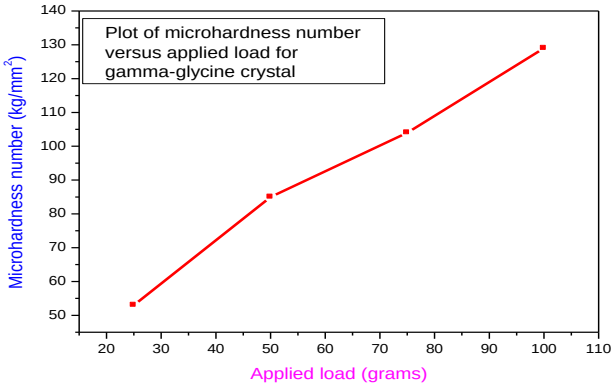

Fig.12: Plot of Vickers microhardness number with applied load for gamma-glycine crystal

Meyer's law is given by $P = kd^n$, where k is the resistance of the material to initial penetration and P is load, n is the work hardening coefficient, P is the load and d is the average diagonal indentation length. Laboratory of Eugene Meyer of the Materials Testing at the Imperial School of Technology in Germany developed this expression in 1908. Meyer's index serves as a gauge of the deformation's impact on the crystal's hardness. The slope is determined by drawing a graph of log(P) against log(d), as shown in figure 13 and the obtained value of n for gamma-glycine crystal is 5.355. Since this value is more than 1.6, the prepared gamma-glycine crystal is found to be a soft material[35].

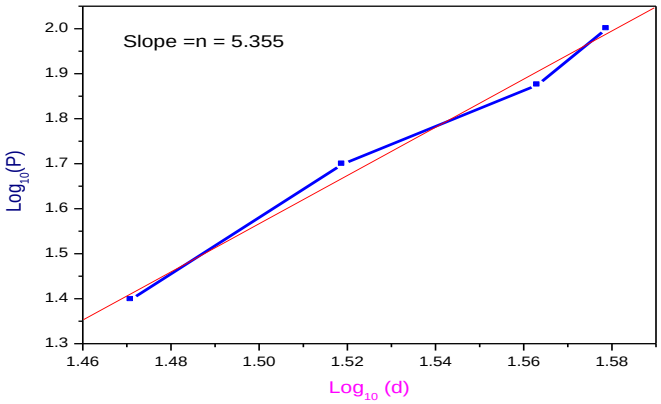

Fig.13: Meyer's plot for gamma-glycine crystal

TG/DTA analysis

The thermogravimetric (TG) and DTA analyses of the grown gamma-glycine crystal were carried out between 20-750 ºC in the nitrogen atmosphere at heating rate of 20˚C/min, using SIMULTANEOUS DTA – TGA, NO 650 – 414 thermal analyser, to find out the thermal stability of the grown GG crystal and the recorded thermal curves of the sample are shown in the figures 14 and 15. TG curve exhibits no change in weight upto 260 ºC, which eliminates the feasibility of solvent formation of the crystal. The major weight loss of 6.6% in TG curve from 260 to 300 ºC suggests the decomposition and sublimation of γ – glycine single crystal. And then the second weight loss of 18.5% from 300 to 475 ºC suggests the further decomposition of the sample. The remaining sample melts and evaporates and it gives a overall weight loss percentage of 22.5% from 475-720 ºC. This suggests that the grown crystal possesses excellent thermal behavior which is a remarkable criteria for NLO applications. The DTA shows a major endothermic peak at 265˚C and it corresponds to the decomposition point of gamma-glycine crystal. It is also found that the sample is thermally stable upto 260 ºC. At elevated temperature this decomposition process continues for a certain time and then the curve gradually decreases. In this present work, the single crystal of γ – glycine is stable upto 260 ºC which contributes for NLO device applications.

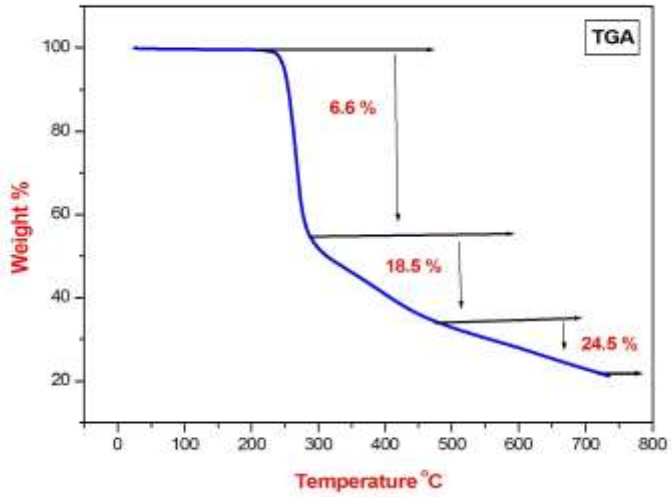

Fig 14: TG curve of the grown gamma glycine crystal

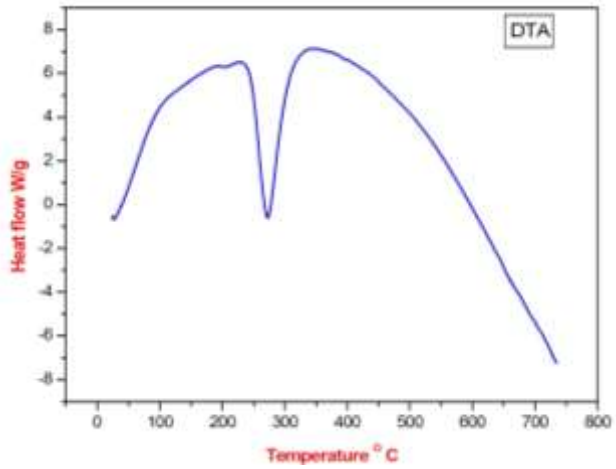

Fig 15: DTA curve for the gamma glycine crystal

CV study

There are three electrodes namely working electrode,
reference electrode, and counter electrode in experimental set-up of cyclic voltammetry (CV). The potential and the current is measured between the working electrode - reference electrode and working electrode - counter electrode respectively. In CV, the potential of the working electrode is swept across a potential range at a constant rate while measuring the resulting current and the characteristic shapes of voltammetry for gamma-glycine (GG) crystalline sample are shown in the figures 16 and 17.

The variation of current with potential for GG crystal was measured the scan rates such as 0.05 V/s and 0.15 V/s. The results indicate that the peak current is more for the scan rate 0.15 V/s than that for 0.05 V/s. For both the scan rates, gamma-glycine (GG) sample shows the complete cycle of voltammograms and hence the sample gives the complete cycle of electrochemical reaction[36].

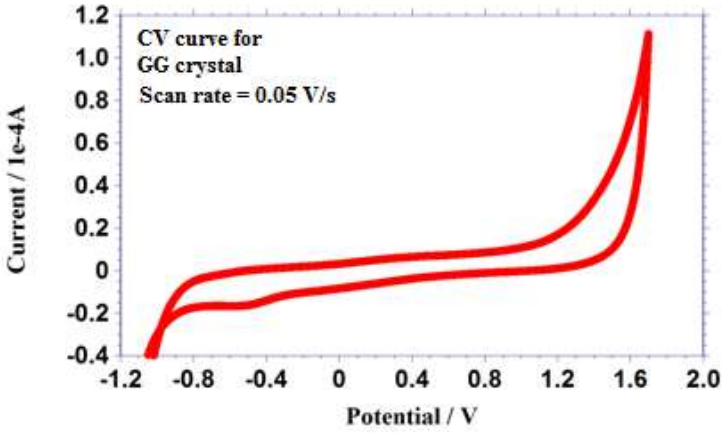

Fig.16: Cyclic voltammetric (CV) curve for GG crystal at the scan rate of 0.05 V/s

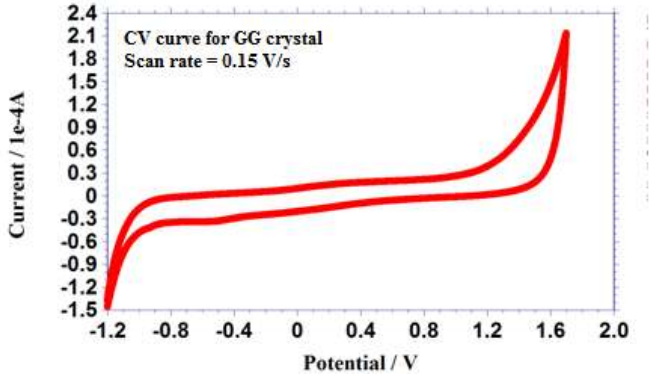

Fig.17: Cyclic voltammetric (CV) curve for GG crystal at the scan rate of 0.15 V/s

Measurement of impedance

Impedance analysis is an effective tool to study the bulk resistance, ac conductivity, dc conductivity and relaxation time of the samples. The complex impedance *Z** defined as $Z^* = Z' - jZ''$ where Z' and Z'' are the real and imaginary components of impedance. The complex impedance of the electrode/insulator/electrode capacitor can be exemplified as the sum of the single RC circuit with parallel combination. The grown crystal of GG is pelletized by using a pelletizer machine and the faces of the sample was coated with the silver paste for getting ohmic contact. The experimental arrangement was electrically shielded and was placed in an electric oven for variation of temperature. The electrodes of the experimental chamber were

connected to an impedance analyzer (IM 6 ZAHNER, Germany) for measuring the real part and imaginary part of impedance of the sample and the measurement was carried out at different frequency values and at 30 ºC and 60 ºC. Figs. 18 and 19 depict the Nyquist's plots for gamma-glycine sample. The values of Z′ in the figures seem to converge at higher frequency. The results show that the values of impedance is more at 30 ºC and it is found to be less at 60 ºC. The grain boundary resistance values of GG crystal at 30 ºC and 60 ºC are 2.4 x 10^4 ohm and 1.7 x 10^4 ohm respectively and hence this sample has negative temperature coefficient of resistance[37,38] .

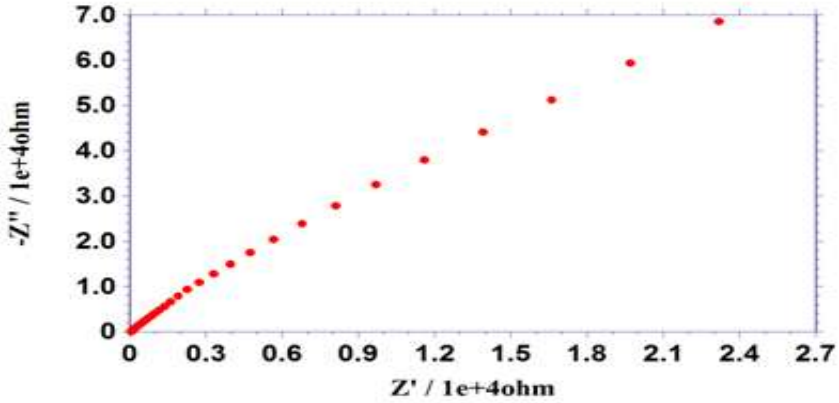

Fig. 18: Nyquist plot for GG crystal at 30 ºC

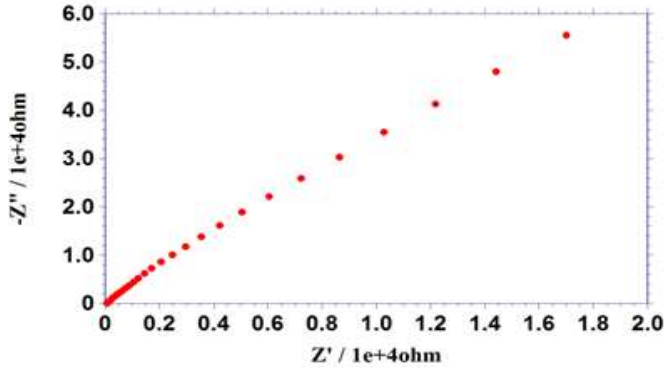

Fig. 19: Nyquist plot for GG crystal at 60 ºC

Antibacterial activity

In order to find out the bacteria and other micro organisms that tend to develop on the surface of the crystalline samples, antibacterial activity is also done and investigated for the grown gamma-glycine crystal. Three bacterial specimens were used for this investigation i.e. Staphylococcus aureus, Pseudomonas aeroginosa and Klebsiella pnemoniae and the areas of zone of inhibition for gamma-glycine (GG) crystal are shown in the figure 20. The estimated values of zones of inhibition are listed in the table 3. From the values, it is clear that the grown GG crystal possess less inhibition against the bacterial pathogens and hence it is concluded that the sample has poorer antibacterial activity against the bacterial specimens[39].

(i) (ii) (iii)

Fig 20: Inhibition areas of gamma-glycine crystal with the bacterial pathogens like (i) Klebsiella pnemoniae, (ii) Staphylococcus aureus and (iii) Pseudomonas aeroginosa

Table 3: Data from the antibacterial activity study for gamma-glycine (GG) crystal

Bacterial specimens	**Zones of inhibition (mm)**	
	GG crystal (mm)	**Standard sample (mm)**
Staphylococcus aureus	12	22
Pseudomonas aeroginosa	12	25
Klebsiella pnemoniae	9	15

3. Conclusion

By using the aqueous solution of cerous chloride, gamma-glycine (GG) crystal was grown in the growth period of about 35 days and transparent, colourless and non-hygroscopic crystal was harvested. The grown crystals of gamma-glycine were subjected to different characterization studies such as structural, optical, infrared, hardness, photoluminescence, impedance, cyclic voltammetric and antibacterial activity studies. Single crystal and powder XRD studies reveal that the GG crystal has hexagonal structure and SHG study indicates that the sample crystallizes in a non-centrosymmetric crystal structure. The various functional groups like CH, NH_3^+, NH, COO^-, CH_2, CCN and CH_2 were found out from the sample by FTIR study. The linear optical parameters such as absorbance, absorption coefficient, optical band gap and extinction coefficient for gamma-glycine crystal were determined by using UV-visible spectral study. The hardness of the sample was measured by applying different loads such as 25 g, 50 g, 75 g and 100 g and the value of work hardening coefficient for GG crystal is found to be 5.355. PL study reveals that GG crystal emits visible and infrared radiation when it is excited with UV light. The various elements present in the sample were identified by using EDAX study. The relative SHG efficiency of gamma-glycine crystal was found to be 1.35 times that of standard KDP sample. Impedance study indicates that GG crystal has negative temperature coefficient of resistance and hence it is an insulating material. The sample was subjected to antibacterial activity study against three bacterial pathogens and it was found that GG crystal has less antibacterial activity. Cyclic voltammetric (CV) study was carried out for the grown crystal of gamma-glycine (GG) at different scan rates and the obtained result reveals that the sample gives the complete cycle of electrochemical reaction. Since the grown gamma-glycine crystal has high SHG efficiency, high mechanical strength, high thermal stability and high transmittance, it could be useful for NLO, laser and opto-electronic applications.

Acknowledgment

The authors are grateful for the research support from various institution such as ACIC - St.Joseph's College, Tiruchirappalli, NCIF - National college, Tiruchirappalli, VOC college, Tuticorin, Cochin University (STIC), Crescent Engineering college, Chenani and Alagappa University, Karaikudi.

Declarations

Author contribution statement

All authors conceived and designed the experiments, performed the experiments, analyzed and interpreted the data.

Data availability statement

The manuscript has data included as electronic supplementary material.

Funding statement

This research did not receive any specific grant from funding agencies in the public, commercial, or not–for–profit sectors.

Competing interest statement

The authors declare no conflict of interest.

4. References

1. Narayanasamy Vijayan, S. Rajasekaran, G. Bhagavannarayana, Ramraj Ramesh, R. Gopalakrishnan, Palanichamy Muthiahpillai and Perumalsamy Ramasamy, Growth and Characterization of Nonlinear Optical Amino Acid Single Crystal: l-Alanine. Crystal Growth & Design , Volume 6 (11), 2006, 2441-2445.
2. J. Uma and V. Rajendran, Growth and characterization of γ-glycine single crystals from cadmium chloride for optoelectronic applications, Optik, Volume 125, Issue 2, 2014, Pages 816-819.
3. Srinivasan Pandurengan, R. Indirajith, R. Gopalakrishnan, (2011), Growth and characterization of α and γ-glycine single crystals, Journal of Crystal Growth, Volume 318 (1), 2011, 762-767.
4. Gustav. Albrecht and Robert B. Corey, The crystal structure of Glycine, Journal of the American Chemical Society, 1939, 61 (5), 1087-1103.
5. L. Li and N. Rodrigues Hornedo, Growth kinetics and mechanism of Glycine crystals, Journal of crystal growth, 121, 1992, pp 33-38.
6. T. Gladys Vimala, E. Bena Jothy and P. Selvarajan, Characterization of Gamma Glycine Crystals Grown Using Rubidium Chloride as an Additive (GGRC),International Journal of Advanced Trends in Engineering and Technology, Volume 2, Issue 1, 2017, Page Number 142-148.
7. D. Arul Asir Abraham, U. Sankar, S. Perumal and P. Selvarajan, Structural analysis of γ – glycine single crystal grown using the aqueous solution of α – glycine and guanidine hydrochloride, International Journal of chemTech Research, Vol 8(1), 2015, pages 105-110.
8. T. Gladys Vimala, E. Bena Jothy and P. Selvarajan, Growth and studies of Gamma glycine crystals doped with zinc sulfate, International Journal of engineering and applied sciences, Vol 3(1), 2016, pages 53-56.
9. T. Gladys Vimala, E. Bena Jothy and P. Selvarajan, Studies of gamma glycine crystals grown in the aqueous solution of cesium chloride, IOSR Journal of Applied Physics, 2017, pages 26-30.
10. R.S.A. Almufarij, A.E.-D. Ali ; M.E. Elba, H.E. Okab, O.M. Mailoud, H. Abdel-Hamid, H.A. Fetouh Elsayed, Growth of New, Optically Active, Semi-Organic Single Crystals Glycine-Copper Sulphate Doped by Silver Nanoparticles, Appl. Nano 2023, 4, 115–137. https://doi.org/10.3390/ applnano4020007
11. T. Bharani raj and P. Philominathan, Growth and Characterization of gamma glycine single crystals grown from alpha glycine in the presence of sodium acetate, Journal of Minerals and Materials Char. & Engg., 10(4), 2011, 351-356.
12. A. Arputha Latha, M. Anbuchezhiyan, C. Charles Kanakam and K. Selvarani, Synthesis and characterization of γ-glycine – a nonlinear optical single crystal for optoelectronic and photonic applications, Materials Science-Poland 35 (2017): 140 - 150.
13. R. Ashok kumar, R. Ezhil Vizhi, N. Siva kumar, N. Vijayan, D. Rajan babu, Crystal growth, optical and thermal studies of nonlinear optical γ-glycine single crystal grown from lithium nitrate, Optik, 123(5), 2012, 409-413.
14. S. Anbuchudar Azhagan and S. Ganesan, Growth and Characterization of gamma glycine single crystals from ammonium sulfate as solvent, Recent Research in Sci & Tech., 2(6), 2010, 107-109.
15. M. Esthaku Peter and P. Ramasamy, Growth of Gamma Glycine Crystal and Its Characterisation, Spectrochimica Acta Part A: Molecular and Biomolecular Spectroscopy , Vol 75 (5), (2010), 1417–1421.
16. VJ. Priyadharshini, A. Meharaj Begum, P. Baby shalini and G. Meenakshi, Growth and study of gamma glycine mixed with oxalate, nitrate and maleic acid, with its structure and transmission by SEST method, 19 September 2022, PREPRINT (Version 1) available at Research Square
17. J. Uma and V. Rajendran, Growth and characterization of γ-glycine single crystals from cadmium chloride for optoelectronic applications, Optik, 125(2), 2014, 816-819.

18. T. P. Srinivasan, R. Indrajith and R. Gopalakrishnan, Growth and Characterization of γ – glycine single crystals, Journal of crystal growth, 318, 2011, 762-767.
19. Eckehard Mueller, The Debye–Scherrer technique – rapid detection for applications. Open Physics, 20(1), 2022, 888-890.
20. Dr. Tiwari, Shreya Talreja, Powder x-ray crystallography-a powerful tool of analysis and identification, The International journal of analytical and experimental modal analysis, 12, 2020, 109-116.
21. A. ltomare, Corrado Cuocci, G.D. Gatta, Anna Moliterni, Rosanna Rizzi, Methods of crystallography: powder X-ray diffraction. 2017.
22. P. Surya and M. Mary Freeda, Studies on the growth and characterization of pure and thiourea doped Triglycine zinc sulphate single crystals, International Journal for research in emerging science and technology, 3(2), 2016, 29-34.
23. M. Udhaybhaskar, S. Senthilkumar and G. Shankar, Growth and characterization of ammonium chloride inorganic crystals modified by thiourea bandgap measurement and structural parameters study for future scope in photonics and optoelectronics, Advances and applications in mathematical sciences, 21(6), 2022, 3503-3514.
24. S. Supriya, S. Kalainathan, G. Bhagavannarayana, Effect of KOH on glycine phosphate single crystal grown by the SR method, Journal of physics and chemistry of solids, 74, 2013, 70-74.
25. V. Vidhya, R. Muraleedharan, Ramajothi and G. vinitha, Structural and optical studies of glycine based single crystals – a nonlinear optical material, European Journal of molecular & clinical medicine, 7(4), 2020 , 2622-2633.
26. Govinda Verma and Dr. Manish Mishra, Development and Optimization of UV-Vis Spectroscopy – a Review, World Journal of Pharmaceutical Research, 7(11), 2018, pg 1170-1180.
27. Dipali Atole and Hrishikesh Rajput, Ultraviolet spectroscopy and its pharmaceutical applications- A brief review, Asian Journal of Pharmaceutical and Clinical Research, 11, 2018, 59.
28. Smit Patel , Aniket Raulji , Diya Patel , Diya Panchal, Prof. Mitali Dalwadi , Dr. Umesh Upadhyay, A Review on UV Visible Spectroscopy, International Journal of Pharmaceutical Research and Applications, 7(5), 2022, 1144-1151.
29. A. Suba, P. Selvarajan, J. Jebaraj Devadasan, Rubidium chloride doped magnesium oxide nanomaterial by using green synthesis and its characterization, Chemical physics letters, 793, 2022, 139463.
30. Manuel Scimeca, Simone Bischetti, Harpreet Lamsira, Rita Bonfiglio, and Elena Bonanno, Energy Dispersive X-ray (EDX) microanalysis: A powerful tool in biomedical research and diagnosis. European journal of histochemistry: EJH, 62, 2018, 2841.
31. George Vander Voort and Gabriel Lucas, Microindentation hardness testing. Metal Progress., 1988, 154, 21-25.
32. S. Sivapriya, K. Balasubramanian, Studies on growth and physical properties of Piperazinium nitrate semi organic single crystal, Eur. Chem. Bull. 2023, 12 (S2), 495 – 502.
33. M Lakshmipriya, D. Babu, R. Ezhil Vizhi, Vickers microhardness studies on solution-grown single crystals of potassium boro-succinate, IOP Conference Series: Materials Science and Engineering, 73, 2015, 012091.
34. Susmita Karan, S.P. Sen Gupta, Vickers microhardness studies on solution-grown single crystals of magnesium sulphate hepta-hydrate, Materials Science and Engineering: A, Volume 398 (1–2), 2005, 198-203.
35. K Sangwal, Microhardness of as-grown and annealed lead sulphide crystals. J Mater Sci 24, 1128–1132 (1989). https://doi.org/10.1007/BF01148809
36. E.E. Kalu, T.T. Nwoga, V. Srinivasan, J.W. Weidner, Cyclic voltammetric studies of the effects of time and temperature on the capacitance of electrochemically deposited nickel hydroxide, Journal of Power Sources, Volume 92, Issues 1–2, 2001, Pages 163-

167. https://doi.org/10.1016/S0378-7753(00)00520-6
37. J.R. Macdonald, Impedance Spectroscopy, Emphasizing solid materials and system, Wiley Interscience Pub., 1987, Newyork.
38. Tushar Kanti Bera, Electrical Impedance spectroscopy for photovoltaic materials: Possibilities and challenges, IOP Conf. Ser.: Mater. Sci. Eng. 955, 012076, 2020, https://doi.org/10.1088/1757-899X/955/1/012076
39. S. Vasumathi, H. Johnson Jeyakumar and P. Selvarajan, Growth, Spectral, NLO, hardness, Hirshfield and antibacterial activity studies of melaminium cyanoacetate monohydrate crystals, Journal of molecular structure, 1263, 2022, 133158.